



POLİTEKNİK DERGİSİ

*JOURNAL of POLYTECHNIC*

ISSN: 1302-0900 (PRINT), ISSN: 2147-9429 (ONLINE)

URL: <http://dergipark.org.tr/politeknik>



# Numerical calculations for the length of the transitory zone in partially filled circular pipes with steep slope

*Kısmen dolu yüksek eğimli dairesel borularda geçiş bölgesi uzunluğunun sayısal olarak hesaplanması*

*Yazar(lar) (Author(s)):* Kenan KAYA<sup>1</sup>, Oktay ÖZCAN<sup>2</sup>

*ORCID<sup>1</sup>:* 0000-0002-6897-4077

*ORCID<sup>2</sup>:* 0000-0002-6836-3831

**To cite to this article:** Kaya K. ve Özcan O., “Numerical Calculations for the Length of the Transitory Zone in Partially Filled Circular Pipes with Steep Slope”, *Journal of Polytechnic*, \*(\*) : \*, (\*).

**Bu makaleye şu şekilde atıfta bulunabilirsiniz:** Kaya K. ve Özcan O., “Numerical Calculations for the Length of the Transitory Zone in Partially Filled Circular Pipes with Steep Slope”, *Politeknik Dergisi*, \*(\*) : \*, (\*).

**Erişim linki (To link to this article):** <http://dergipark.org.tr/politeknik/archive>

**DOI:** 10.2339/politeknik.1521326

# Numerical Calculations for the Length of the Transitory Zone in Partially Filled Circular Pipes with Steep Slope

## Highlights

- ❖ The length of the transitory zone in circular open channels is investigated numerically.
- ❖ Effect of several parameters such as the Reynolds number, Froude number and filling ratio at the pipe inlet; as well as the pipe slope is investigated.
- ❖ The transitory length shows a tendency to decrease with the Reynolds number, contrary to the entrance length in pipe flow.
- ❖ Numerical calculations predict that uniform open channel flow is guaranteed approximately 110 and 60 diameters downstream the inlet, for smooth and corrugated circular pipes, respectively.

## Graphical Abstract

The length of the transitory zone in partially filled circular smooth and corrugated pipes is investigated numerically. Effect of several parameters such as the Reynolds number, Froude number and filling ratio at channel inlet; as well as the channel slope is investigated.

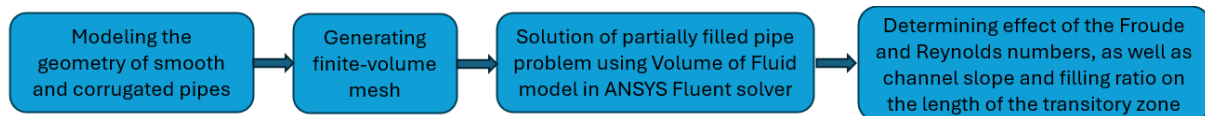


Figure. Workflow adopted in the present study

## Aim

It is aimed to numerically investigate the effects of parameters such as Reynolds number, Froude number, filling rate and channel slope on the length of the transitory zone in partially filled circular smooth and corrugated pipes.

## Design & Methodology

Using the ANSYS Fluent solver, the two-phase flow in the pipe is solved by the Volume of Fluid method, and the length of the transitory zone is calculated by obtaining the free surface profile.

## Originality

It has been revealed that there is no consensus regarding the length of the transitory zone in the relevant literature. It is thought that the current study will partially address the gap in this field.

## Findings

Results of the numerical calculations show that uniform open channel flow is guaranteed roughly 110 and 60 diameters downstream the pipe entrance, for smooth and corrugated pipes, respectively.

## Conclusion

Variation of the length of the transitory zone with the Reynolds and Froude numbers, filling ratio, and slope is presented in tables and graphs, and the results are discussed.

## Declaration of Ethical Standards

The author(s) of this article declare that the materials and methods used in this study do not require ethical committee permission and/or legal-special permission.

# Numerical Calculations for the Length of the Transitory Zone in Partially Filled Circular Pipes with Steep Slope

*Araştırma Makalesi / Research Article*

Kenan KAYA<sup>1\*</sup>, Oktay ÖZCAN<sup>2</sup>

<sup>1</sup>Department of Mechanical Engineering, Istanbul Aydın University, 34295, Istanbul, Turkey

<sup>2</sup> Department of Aeronautical Engineering, Faculty of Engineering and Architecture, Istanbul Gelisim University, 34310, Istanbul Turkey

(Geliş/Received : 23.07.2024 ; Kabul/Accepted : 03.03.2025 ; Erken Görünüm/Early View : 27.04.2025 )

## ABSTRACT

Three-dimensional turbulent free-surface flow through smooth and corrugated circular pipes with steep slope is simulated by means of Computational Fluid Dynamics (CFD). For this purpose, the three-dimensional Reynolds Averaged Navier-Stokes equations are solved using the ANSYS *Fluent* solver, while interface between air and water is calculated using the *Volume of Fluid* (VOF) method. Effect of inlet conditions regarding the Froude and Reynolds numbers, channel slope and filling ratio on the length of flow development is investigated while both sub-critical and super-critical inlet conditions are considered. Results of the numerical calculations show that uniform open channel flow is guaranteed roughly 110 and 60 diameters downstream the pipe inlet, for smooth and corrugated pipes, respectively. The transitory length shows a tendency to decrease with the Reynolds number, contrary to the entrance length in pipe flow.

**Keywords:** Uniform open-channel flow, smooth pipe, corrugated pipe, computational fluid dynamics, volume of fluid method.

## Kısmen Dolu Yüksek Eğimli Dairesel Borularda Geçiş Bölgesi Uzunluğunun Sayısal Olarak Hesaplanması

ÖZ

Yüksek eğimli pürüzsüz ve oluklu dairesel borulardaki üç boyutlu türbülanslı serbest yüzey akışı Hesaplamalı Akışkanlar Dinamiği (HAD) aracılığıyla hesaplanmıştır. Bu amaçla üç boyutlu Reynolds Ortalamalı Navier-Stokes denklemleri ANSYS *Fluent* yazılımı kullanılarak çözülürken, hava ve su arasındaki arayüzey *Volume of Fluid* (VOF) yöntemi kullanılarak hesaplanmıştır. Froude ve Reynolds sayıları, kanal eğimi ve doluluk oranına ilişkin giriş koşullarının akış gelişim uzunluğuna etkisi araştırılmış, kritik-altı ve kritik-üstü giriş koşulları göz önünde bulundurulmuştur. Sayısal çözüm sonuçları, dairesel pürüzsüz ve oluklu borular için boru girişinden akım altı yönünde yaklaşık 110 ve 60 çap mesafede üniform açık kanal akışının garanti edilebileceğini göstermektedir.

**Anahtar Kelimeler:** Üniform açık kanal akışı, pürüzsüz boru, oluklu boru, hesaplamalı akışkanlar dinamiği, volume of fluid yöntemi.

## 1. INTRODUCTION

Transitory zone, or transitory reach, is defined as the streamwise distance from the channel inlet up to the cross-section at which uniform flow is established [1]. Establishment of uniform flow is necessary for some discharge calculation methods; that is, employing a uniform flow formula such as Manning or Chezy, or the end-depth ratio (EDR). These methods require that the relevant characteristics of a given channel (resistance coefficient or EDR) are determined experimentally (or analytically) in advance under the assumption of uniform flow conditions, and then discharge is calculated again in a control section where uniform flow is assumed to prevail. Therefore, in such applications especially involving artificial channels stream-wise extent of the transitory zone must be known to determine the

minimum required channel length for flow to become uniform.

A free surface flow with the depth and mean velocity not changing in the flow direction is known as uniform flow, a more strict and idealized definition of which dictating that the velocity profile must be unchanged over a cross section of flow [1]. In that respect, uniform flow relates to fully developed flow in ducts and pipes. It is rather simple to distinguish the laminar fully developed flow in ducts by monitoring some features of the mean flow variables, that is, constant values of the centerline velocity and wall shear stress, and linear pressure gradient, which result from an invariant velocity profile corresponding to that of Hagen-Poiseuille flow [2]. For fully developed turbulent flows in ducts, prevalence of a logarithmic mean velocity distribution is taken into

\*Sorumlu Yazar (Corresponding Author)  
e-Posta : kenankaya@aydin.edu.tr

consideration; however, higher-order turbulence statistics, which are too sensitive to inlet conditions, do not develop simultaneously with the mean flow variables [3]. It has been shown by previous experiments, that near the bottom wall in an open channel flow the velocity profile still complies with the logarithmic law of the wall of a flat plate boundary layer to a large extent, however, it shows somewhat different characteristics in the outer region of the boundary layer, attributed to the free surface which suppresses the turbulent stress in the wall-normal direction and leads to anisotropic turbulence [4 - 7].

Information about the minimum required channel length for uniform flow to establish, i.e., the transitory zone ( $L_e$  in the following), is scarce in the relevant literature. Despite the aforementioned dissimilarities, Knight [8], in his previous experimental work to obtain boundary shear stress in partially full circular pipes under subcritical and supercritical flow regime, assumed fully developed circular open-channel flow for  $x/4R > 60$  ( $R$ : hydraulic radius), referring to that the fully developed turbulent pipe flow would occur for  $x/D > 60$  ( $D$ : pipe diameter). Likewise, Nezu and Rodi [4] stated that their channel length satisfied the necessary condition of  $x/4R \geq 60$  to have uniform flow in their experimental study, where they investigated the fully developed turbulent velocity profile in rectangular open channel flow and compared them with the well-known logarithmic law of the wall. Balachandar et al. [5] studied open-channel flow in a rectangular flume for a range of subcritical and supercritical Froude numbers using a laser Doppler anemometer and measured the turbulent velocity profile. They assumed fully developed turbulent boundary layer approximately 50-70 flow depth downstream the channel inlet.

Although they do not explicitly refer to  $L_e$ , it might also be useful to cite some previous studies which have proposed a minimum length for subcritical approach flow in a free overfall, which is used as a flow measuring device by employing the EDR method [9-12]. According to this method, discharge is calculated employing an energy equation derived from the Bernoulli equation, that involves the critical depth,  $h_c$ , and assumes hydrostatic pressure distribution, which is characteristic of uniform open channel flow [9]. Therefore, for accurate calculation of discharge, the approach flow must be uniform. In case of supercritical approach flow, the normal depth,  $h_n$ , is used as reference depth instead, which still requires the establishment of uniform flow [9, 13]. Here, the EDR of a given overfall structure is already known, so that  $h_c$  and  $h_n$  can be calculated by measuring

the flow depth at the brink. Table 1 presents some proposed values of minimum length for subcritical rectangular approach flow in a free overfall, in terms of  $h_c$ , which reveals the disagreement on  $L_e$ . Bauer and Graf [14] conducted experiments to investigate EDR in a free overfall with approaching flow of mild slope, i. e., subcritical flow, where they reported that an approach channel of  $20h_c$  length, as proposed by Carstens and Carter [10], was not enough to achieve uniform flow conditions, and therefore, they failed to establish uniform flow due to insufficient channel length. To the authors' knowledge, Rajaratnam and Muralidhar [15] and Bos [11] are the only work proposing a minimum required length for achieving uniform flow in partially filled circular pipes: Rajaratnam and Muralidhar [15] conducted an experimental study on free overfall in horizontal and sloping circular pipes and applied momentum analysis on the flow to obtain an expression for the EDR. They stated that a minimum pipe length of  $20H_0$  is required upstream of the pipe exit for discharge measurement using the EDR method with subcritical approach flow, where  $H_0$  denotes the energy head at any section within the uniform flow zone. Bos [11] proposed a minimum pipe length of  $6D$  for proper application of EDR method in horizontal circular channels but did not mention sloped circular pipes.

Reynolds and Froude number dependence of flow development length in rectangular open channels has been investigated by some previous studies. Results of the experimental study conducted by Kirkgöz and Ardiçlioğlu [16] indicated that, the length of developing flow zone is a decreasing linear function of another dimensionless parameter,  $Re/Fr$  (calculated in the region of uniform flow), in case of subcritical flow in rectangular channels (for  $0.3 < Fr < 0.7$  and  $28000 < Re < 137000$ ). They specified the onset location of developed flow qualitatively, observing the velocity profiles and flow depth. Contrarily, Ranga Raju et al. [17] stated that  $L_e$  does not depend on the Froude number, according to results of their numerical calculations for subcritical rectangular open-channel flow; but it does on the Reynolds number in an exponential fashion and flow aspect ratio in case of smooth flow, and only on the relative roughness and aspect ratio in case of rough flow (for  $0.1 < Fr < 0.6$  and  $5100 < Re < 30600$ ). Numerical simulations conducted by Bonakdari et al. [18] on turbulent flow in smooth and rough rectangular open channels demonstrated that  $L_e$  is inversely proportional to the Reynolds number, while the Froude number does not seem to influence  $L_e$  both in smooth and rough rectangular channels. A previous experimental study by

**Table 1.** Some proposed values of minimum length required for uniform flow to be established in subcritical rectangular approach channel of a free overfall

Reference	Minimum required length of approach channel[m]
Subramanya [9]	$15h_c$
Carstens and Carter [10]	$20h_c$
Bos [11]	$12h_c$
Ferro [12]	$55h_c$

Wilkerson et al. [19] indicated that  $L_e$  does not depend on the Reynolds and Froude numbers for rough channels with rectangular cross-section. The reason for the contradiction about the dependence on the Froude and Reynolds numbers between different studies is unclear.

It is important to have uniform – or, so-called fully developed – flow for studying turbulent velocity profile, or measuring the flow rate in open channel flows. However, the literature review presented above reveals that there is not a systematic investigation on the required length for uniform flow to establish,  $L_e$ , in circular open channels, although it is well established for pressurized flow in ducts. The novelty of this study is that it attempts to close this gap by proposing a method to estimate  $L_e$  of subcritical and supercritical open channel flows in circular smooth and corrugated pipes for various combinations of some dynamic parameters such as Froude and Reynolds numbers, flow depth and filling ratio at the inlet, using the methods of computational fluid dynamics. As a geometrical parameter, the effect of slope is also investigated. This study also differs from previous studies in that control parameters such as the Reynolds and Froude numbers are calculated at the channel inlet section rather than in the uniform flow region. Contrary to the entrance length in pipe flow, the transitory zone in circular open channels promises much more difficulty; since, owing to the existence of free surface, there are additional variables such as flow depth and the Froude number which may possibly have effect. Using computational fluid dynamics has the advantage over experimental methods, that it is possible to satisfy both Reynolds and Froude number similarity simultaneously between distinct cases of open-channel flow by employing imaginary fluids.

## 2. NUMERICAL METHOD

### 2.1. Governing Equations

Computational fluid dynamics (CFD) has emerged since the governing equations of fluid flow are non-linear partial differential equations and their general solution cannot be obtained analytically. Moreover, even when the equations in question are simplified by linearizing them employing various assumptions, analytical solutions are quite difficult for problems with complex geometry. CFD is a relatively new method that has developed in addition to the analytical and experimental methods used in research, development and design studies in the discipline of fluid mechanics and has become increasingly used for academic and industrial purposes in parallel with the rapid increase in the processing power of computers used in calculations. Numerical solution methods, which constitute the subject of CFD, deal with solving the governing equations, which include partial derivatives and are written primarily for continuum, by converting them into a system of algebraic equations expressed on a discrete domain to comply with certain constraints.

It is a reasonable simplification to assume that the open channel flow in underground drainage systems is a two-phase flow consisting of immiscible water and air phases. Specific numerical methods which are used to capture discontinuities (e.g. shock waves) can also be used to capture the interface of immiscible fluids. Hyman [20] mainly classified these methods as interface tracking, volume tracking and moving mesh methods. In interface tracking methods, the position of marker points representing the free surface is calculated by a height function or parametric curve interpolation. In volume tracking methods, not only the free surface but also the entire volume occupied by the selected phase or phases is determined by marking. The MAC (Marker and Cells) method is one of those methods, where a transport equation is solved to determine the position of the marker particles once a single set of equations for the field variables such as velocity and pressure are solved for all phases [21]. In this study, the Volume of Fluid (VOF) [22] method, which is a volume tracking method based on the MAC method, is used. In this method, in addition to the continuity and momentum equations, the advection equation for the volume fraction is solved, which is given by Eq. (1):

$$\frac{\partial F}{\partial t} + u_k \frac{\partial F}{\partial x_k} = 0 \quad (k = 1, 2, 3) \quad (1)$$

Here the volume fraction is represented by step function  $F$ , which is equal to unity for cells containing a selected fluid phase in the domain, and zero otherwise. The three-dimensional, incompressible and unsteady conservation equations of mass and momentum (i.e., the Navier-Stokes equations) are given in Eqs. (2) in conservative form with index notation, as follows:

$$\frac{\partial(\rho u_k)}{\partial x_k} = 0 \quad (i = k = 1, 2, 3) \quad (1a)$$

$$\frac{\partial(\rho u_i)}{\partial t} + \frac{\partial(\rho u_i u_k)}{\partial x_k} = -\frac{\partial p}{\partial x_i} + \mu \frac{\partial^2 u_i}{\partial x_k^2} \quad (2b)$$

Here  $u_i$  and  $x_i$  represent components of the velocity (m/s) and position (m) vectors, respectively.  $t$  is time (s),  $\rho$  and  $\mu$  are the density ( $\text{kg/m}^3$ ) and dynamic viscosity ( $\text{kg/ms}$ ) of the fluid, respectively,  $p$  is the pressure ( $\text{N/m}^2$ ), and  $f_i$  expresses components of the conservative force ( $\text{N/m}^3$ ) acting on the unit fluid volume.

### 2.2. Interpolation Methods for the Volume Fraction

In the VOF method, regions where the volume fraction function ( $F$ ) takes a value between 0 and 1 indicate the free surface. The  $F$  function takes the value 1 on one side of the cells representing the interface and 0 on the other side. There is indeed discontinuity for the volume fraction at the interface, and therefore, discretization of the convective acceleration term ( $u_k \partial F / \partial x_k$ ) in the transport equation of the volume fraction (Eq. (1)) requires the development of improved interpolation methods since the conventional upwind and central difference methods yield extremely diffusive, oscillatory and unconstrained results [23]. For this purpose, nonlinear high-resolution methods obtained by applying a limiter to interpolation methods of at least second-order

accuracy can be used to capture regions of discontinuity [24]. HRIC (*High Resolution Interface Capturing*) method is one of these interpolation methods, where the limiting criterion is achieved by applying the Normalized Variable (NV) approach [25].

In Fig. 1, comparison of some interpolation methods available in the commercial ANSYS Fluent 15 code are presented, where contours of the volume fraction in a free fall are given. Regions of dark color indicate the free surface where the volume fraction takes values between 0 and 1. In case of the First Order Upwind (FOU) interpolation is used, the free surface is quite thick due to numerical diffusion (Fig. 1a). On the other hand, a relatively sharper free surface is obtained with Second Order Upwind (SOU) interpolation (Figure 1b). Fig. 1c shows that the CICSAM (Compressive Interface Capturing Scheme for Arbitrary Meshes) method [26], being another high-resolution interpolation method, produces a very sharp free surface, however, oscillations occur near the free surface. The HRIC method calculates a free surface that has a similar level of sharpness with much less deformation than that obtained by the CICSAM method (Fig. 1d). Here, all the other parameters such as the numerical grid and time step are the same for all four numerical solutions presented.

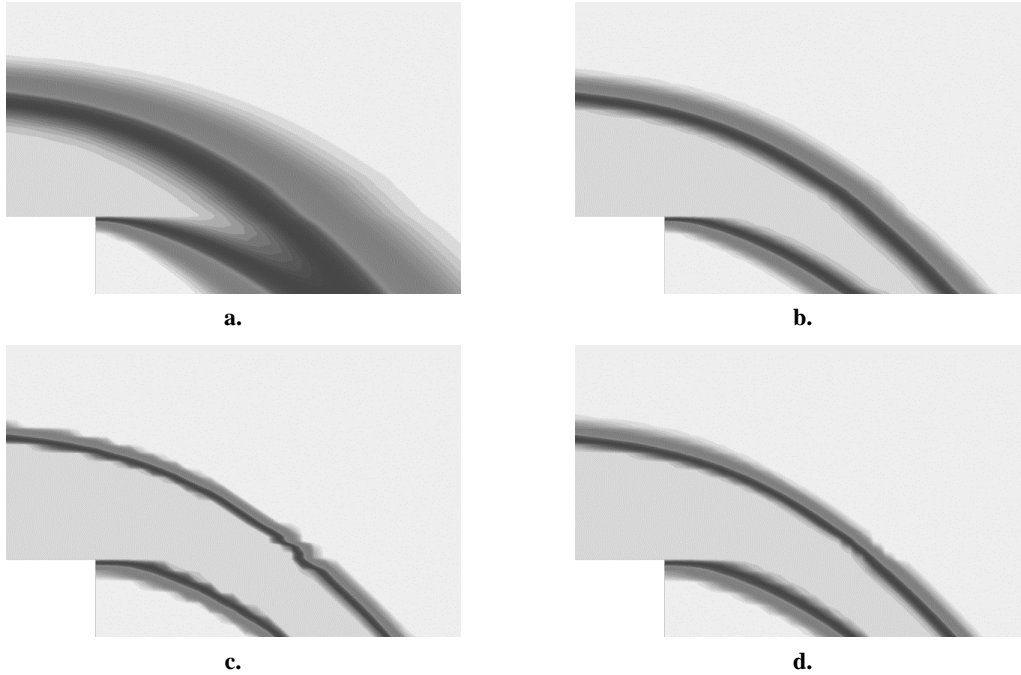


**Figure 1.** Contours of volume fraction obtained by the interpolation methods: a) FOU, b) SOU, c) CICSAM, and d) HRIC

### 2.3. Data Reduction

The geometrical parameters related to a partially full circular pipe are shown in Fig. 2. Accordingly,  $A$  and  $P$  denote the cross-sectional area of the flow (the hatched area), and the wetted perimeter (shown with a thick arc along the bottom part of the pipe), respectively; while  $D$  and  $R$  are the inner diameter and radius of the pipe,  $h$  is the flow depth, and  $b$  is the width of the free surface. It should be noted here that the wetted perimeter,  $P$ , does

not include the free surface. An angle parameter,  $\alpha$ , which depends on  $h$  and  $R$  and given by Eq. (4) below, is also introduced:

$$\alpha = \cos^{-1} \left( 1 - \frac{h}{R} \right) \quad (4)$$

$A$ ,  $P$  and  $b$  can be related to  $R$  and  $\alpha$ , as given by Eqs. (5), (6) and (7):

$$A = R^2 (\alpha - \sin \alpha \cos \alpha) \quad (5)$$

$$P = 2\alpha R \quad (6)$$

$$b = 2R \sin \alpha \quad (7)$$

The hydraulic radius,  $R_h$ , is defined as the ratio of the cross-sectional area of the flow to the wetted perimeter, i. e.,  $R_h = A/P$ . Thus, substitution of Eqs. (5) and (6) in the definition of  $R_h$  yields Eq. (8):

$$R_h = R \frac{(\alpha - \sin \alpha \cos \alpha)}{2\alpha} \quad (8)$$

The filling ratio of the pipe is defined as ratio of the flow depth,  $h$ , to the pipe diameter,  $D$ . The Reynolds number is based on the hydraulic radius,  $R_h$ , and the cross-sectional average velocity,  $U$ , which is given by Eq. (9):

$$Re = \frac{\rho U R_h}{\mu} \quad (9)$$

where  $\rho$  and  $\mu$  are density and dynamic viscosity of the fluid, respectively.

The Froude number is defined by Eq. (10) below:

$$Fr = \frac{U}{\sqrt{g h_m}} \quad (10)$$

Here  $g$  is the gravitational acceleration, and  $h_m$  is the hydraulic mean depth, which is the ratio of the cross-sectional area of flow,  $A$ , to the width of the free surface,  $b$ ; and can be expressed in terms of  $R$  and  $\alpha$ , as given by Eq. (11):

$$h_m = R \frac{(\alpha - \sin \alpha \cos \alpha)}{2 \sin \alpha} \quad (11)$$

## 2.4. Solution Domain, Numerical Grid and Boundary Conditions

The smooth and corrugated pipes considered in this study are shown in Fig. 3a and 3b, respectively. Inner configuration of the corrugated pipe and the related parameters are also shown in Fig. 3b. Accordingly,  $r$  and  $L$  denote amplitude and wavelength of corrugations, respectively; and  $D$  is the pipe diameter. In all the numerical calculations regarding the corrugated pipe, the ratio of  $r/L$  and  $r/D$  is kept constant at 0.1 and 0.01, respectively.

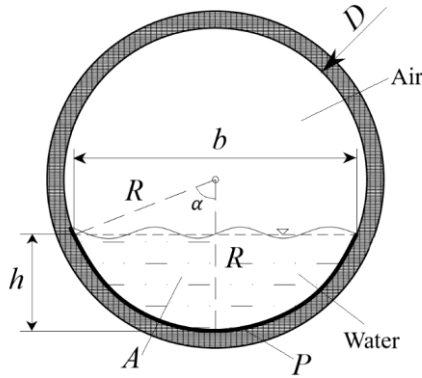


**Figure 2.** Illustration of the geometrical parameters related to a partially filled circular pipe

The solution domain consists of a pipe and a rectangular box at the downstream end of the pipe where the flow is allowed to form a free overfall (Fig. 4a). The reason for including an overfall instead of a pipe exit is the better convergence of the former in the numerical calculations. Only half of the physical domain is considered in the numerical solutions since time-averaged flow is symmetric with respect to the center plane. Pipe lengths vary from  $100D$  to  $200D$  to achieve uniform flow. Boundary conditions are also presented in Fig. 4a. At the pipe inlet, velocity inlet boundary condition is applied for both fluid phases which dictates a fixed uniform velocity profile. Here Phase-1 and Phase-2 represent the gas and liquid phases, respectively. At the bottom face of the rectangular box, where the free-falling jet stream exits the domain, pressure outlet boundary condition is

employed, which sets pressure to zero gauge at the boundary. Symmetry boundary condition is assigned to the center-plane, which forces wall-normal gradients of all flow variables to be zero and corresponds to a slip-wall, i. e., tangential velocity is not zero. Finally, no-slip wall boundary condition is employed at the rest of the boundaries, leading all the velocity components to be zero. Hexahedral elements are generated for the numerical grid, where finer elements are created adjacent to the walls involving the flow of the liquid phase to resolve regions of high velocity gradient near the wall better (Fig. 4b).

## 2.5. Comparison of Turbulence Models

Preliminary numerical calculations have been conducted to compare results obtained by using three different turbulence models, i. e.,  $k-\epsilon$  realizable,  $k-\omega$  SST, and Reynolds Stress Model (RSM). For this purpose, the free-surface flow of water in smooth and corrugated circular pipes of 1 m length is solved numerically, where water is in free fall at the downstream end of the pipe. Parameters related to the preliminary solutions are presented in Table 2, where subscript “0” refers to value of that parameter evaluated at the pipe inlet.

Axial velocity profiles at the outlet section of smooth and corrugated pipes (on the symmetry plane) are presented in Fig. 5a and 5b, respectively, for three different turbulence models. Here,  $u$  represents the velocity component parallel to the channel bed,  $U_0$  denotes cross-sectional average velocity at the pipe inlet,  $y$  is the vertical coordinate, where  $y = 0$  coincides with the channel bed, and  $h_0$  is the flow depth at the pipe entrance. The deviation between the velocity distributions obtained for the turbulence models considered in smooth open channel flow is less than 1% (Fig. 5a). The fact that similar results are obtained with the RSM (Reynolds Stress Model), which does not involve an eddy viscosity approach unlike the  $k-\epsilon$  realizable and  $k-\omega$  SST models, can be explained by the relative simplicity of the problem addressed. The large number of equations of the RSM model (7 additional equations) is a disadvantage, since there is a negligible difference in the velocity profiles. Although the  $k-\epsilon$  realizable and  $k-\omega$  SST models do not have a significant advantage over each other for the flow problem considered among the other turbulence models

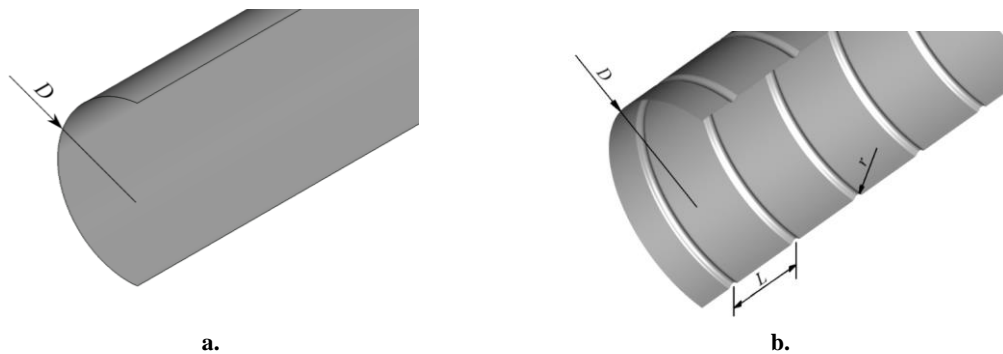


**Figure 3.** Geometry of a) smooth, and b) corrugated pipes along with the relevant geometrical parameters

compared, the  $k-\omega$  SST turbulence model is used in numerical solutions of the smooth open channel flow.

For open channel flow in corrugated pipe, a deviation of at most 10% is observed in the velocity distribution on symmetry plane obtained using different turbulence models for  $y/h_0 < 0.2$  (Fig. 5b). It can be concluded that the reason for this difference is that the flow separation that occurs in the flow over corrugations is a problem that is difficult to predict by turbulence models. It has been reported that the  $k-\omega$  SST model gives good results in boundary layer separation problems with an adverse pressure gradient [27], and therefore  $k-\omega$  SST turbulence model has been used in the corrugated channel flow calculations, as well.

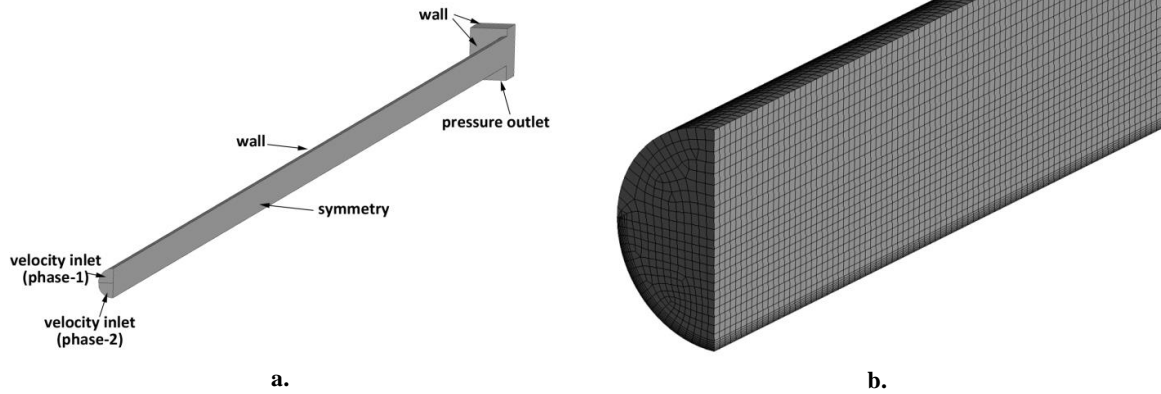


**Figure 4.** Illustration of a) the solution domain and the boundary conditions, as well as b) the numerical grid

## 2.6. Mesh Independence Study

A mesh independence study is conducted by examining the effect of the grid density near the wall, as well as at the air-water interface. Comparison of three different near-wall grids is done for  $y^+ = 5, 10$  and  $30$ , where  $y^+$  is a dimensionless wall distance defined by inner wall variables in the turbulent boundary layer ( $y^+ = u_\tau y / \nu$ ,  $y$ : wall-normal distance,  $u_\tau$ : friction velocity,  $u_\tau = \tau_w / \rho$ ,  $\tau_w$ : wall shear stress,  $\rho$ : fluid density,  $\nu$ : fluid kinematic viscosity). Other parameters related to the mesh independence study are  $D = 0.2$  m,  $L = 1$  m,  $Fr_0 = 2$ ,  $U_0 = 0.693$  m/s,  $S = 0$  and  $Re_0 = 1.98 \times 10^5$ . Velocity profiles plotted at the exit section of the circular pipe are presented in Fig. 6. The deviation between the velocity distributions obtained by employing three different grids near the wall is around 1% at most in smooth channel flow, and less than 5% in corrugated channel flow.

## 2.7. Validation of the Numerical Method

An outline of the numerical scheme adopted in this study is as follows: Time-dependent, incompressible three-dimensional Reynolds Averaged Navier-Stokes (RANS) equations are solved iteratively, with the assumption of constant fluid properties. Multiphase flow is modeled using the Volume of Fluid (VOF) method, where gas-liquid interface is captured by solving a transport equation for volume fraction. The VOF method is applicable only when two fluids are immiscible and form a distinct interface in-between. Since discontinuities in volume fraction take place at the interface; a non-linear high-resolution scheme, that is, the High-Resolution Interface Capturing (HRIC) method, is employed to be able to handle partial derivatives in the transport equation for volume fraction. Menter's  $k-\omega$  turbulence model with Shear Stress Transport (SST) formulation is used

**Table 2.** Parameters related to the numerical solutions using different turbulence models

	$D$ (m)	$h_0/D$	$Fr_0$	$U_0$ (m/s)	$S$	$Re_0$	$L$ (m)
$k-\varepsilon$ realizable							
$k-\omega$ SST	0.2	0.5	0.7	0.693	0.01	$3.5 \times 10^4$	1
RSM							

Accurate calculation of flow depth depends on capturing the free surface with adequate sharpness. For this purpose, an additional calculation is conducted by using an adaptive grid where the elements are locally refined around the free surface, depending on some certain

where  $k$  is turbulence kinetic energy, and  $\omega$  is its specific dissipation [27]. Being one of the eddy-viscosity turbulence models, the  $k-\omega$  SST turbulence model is not capable of capturing the secondary flows, which are well known to affect the flow field in open channels.

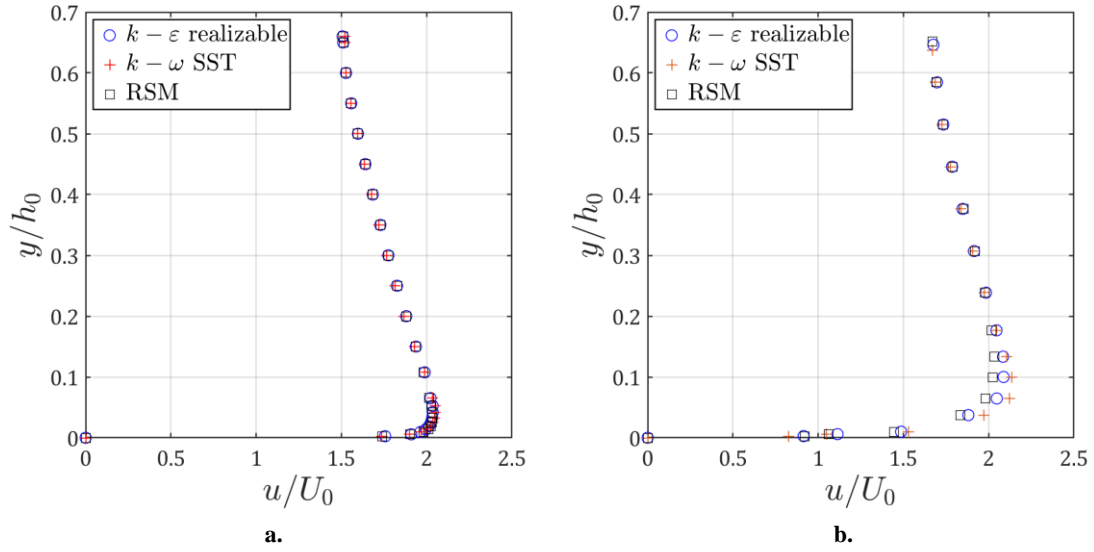


**Figure 5.** Comparison of the velocity profiles at the pipe exit for three different turbulence models for a) smooth, and b) corrugated pipe (on symmetry plane)

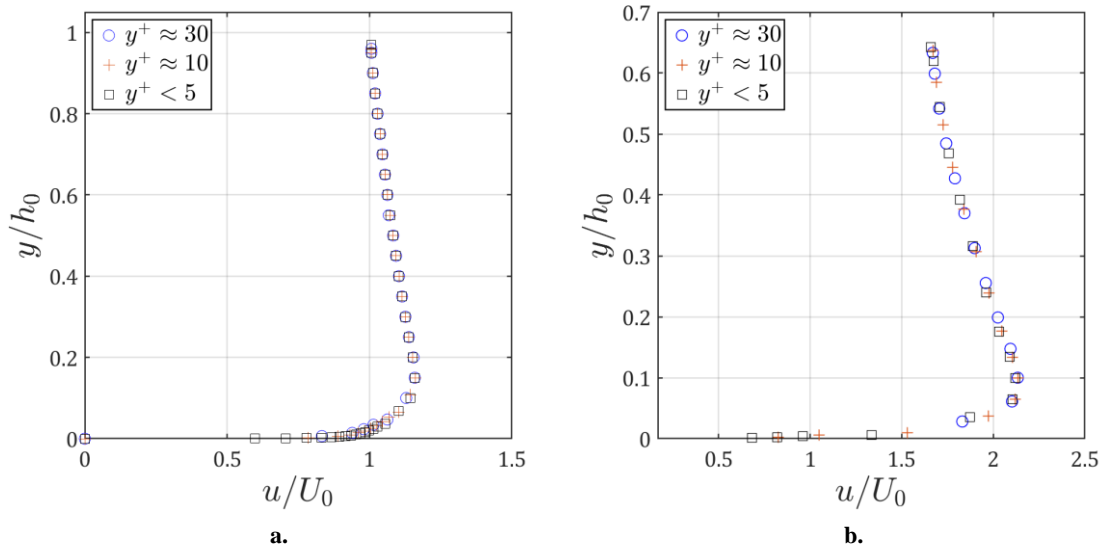


**Figure 6.** Comparison of velocity profiles using three different near-wall grid densities for a) smooth, and b) corrugated pipes

Therefore, in numerical calculations, isotropic turbulence is assumed. Near-wall flow is modeled using wall functions, which assume a logarithmic velocity profile near the wall, since it is computationally too expensive to resolve the whole boundary layer for such a large domain. Second and first order upwind schemes are used for discretization of the nonlinear convective terms in the momentum and turbulence equations, respectively. Pressure-velocity coupling is achieved by the SIMPLE (Semi Implicit Method for Pressure-Linked Equations) algorithm. A gravitational field is imposed on the domain that corresponds to the given slope of the pipe. Solution is assumed to be converged once the maximum percentage change in normal depth ( $h_N$ ) is less than 0.05% per second.

The numerical method employed in this study is validated using a previous experimental study conducted by Kırkgöz and Ardiçlıoğlu [16], where turbulent velocity profiles in a rectangular open channel flow are presented. For comparison purposes, open-channel flow in a smooth rectangular channel of 0.3 m width and 10 m length is solved numerically. Parameters related to the validation study are presented in Table 3. Fig. 8a shows axial velocity profiles at a cross-section of uniform flow, on the symmetry plane. Experimental velocity data at the free surface was not available in [16], which might be due to free-surface waves interrupting laser beams emanating from the Laser Doppler Anemometer (LDA) system [4]. Since a pointwise comparison is a difficult task between the numerical and experimental velocity profiles, integral quantities such as the thicknesses of displacement ( $\delta^* =$

$\int_0^h (1 - u/u_{max}) dy$  and momentum ( $\theta = \int_0^h (u/u_{max})(1 - u/u_{max}) dy$ ) are considered, where the relative error is less than 6% and 15%, respectively for the former and the latter (denoted by  $\varepsilon_{\delta^*}$  and  $\varepsilon_{\theta}$  in Fig. 8a). When the velocity and vertical coordinate are normalized by mean flow variables such as the maximum axial velocity,  $u_{max}$ , and the flow depth,  $h$ , respectively (Fig. 8b); as well as by the wall variables (Fig. 8c), a good collapse of the profiles becomes evident, while both sets of data follow the logarithmic law of the wall quite well. It can therefore be said that the numerical and experimental velocity profiles are similar. The reason for the deviation between the profiles presented in Fig. 8a may be the inlet velocity profile, which is uniform for the numerical calculations, and unclear for the experimental study described in [16].

In Fig. 9a, velocity distributions along the vertical mid-plane of the pipe at various longitudinal locations are presented for a numerical solution conducted for open channel flow in smooth pipe, while Fig. 9b provides a detailed view of the same set of velocity profiles focused on the region near the free surface. As seen in Fig. 9b, the velocity profiles keep developing, albeit with a decreasing rate, in the streamwise direction, and even over a long distance of approximately  $140D$ , the point values of velocity do not remain perfectly constant at different locations, as required by the ideal definition of uniform open-channel flow. Therefore, objectively determining  $L_e$  by observing the development of the velocity profiles is challenging. Instead, if present, the limiting value to which the section-averaged velocity or depth converges can serve as a decisive criterion for identifying  $L_e$ .

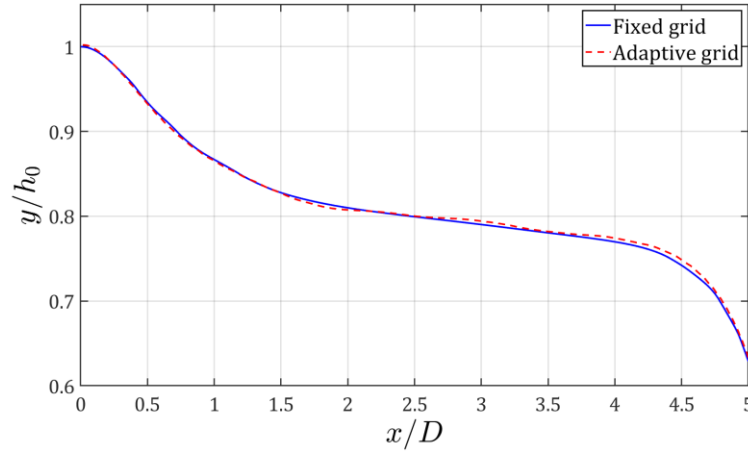


Figure 7. Free surface profiles obtained by using adaptive and non-adaptive grid

Table 3. Parameters related to the validation study [16]

Flow rate, $Q$ [m <sup>3</sup> /s]	Flow depth, $h$ [m]	Flow width, $b$ [m]	Froude number, $Fr$ [-]	Reynolds number, $Re$ [-]
0.006	0.075	0.3	0.31	$1.2 \times 10^4$

### 3. RESULTS AND DISCUSSION

Majority of the data presented in the literature regarding the required distance from the channel entrance to achieve uniform flow, that is,  $L_e$ , pertain to rectangular cross-section channels, and similar results have not been provided for open-channel flow in circular pipes. For this purpose, numerical calculations have been conducted for open channel flow in both smooth and corrugated circular pipes to examine the variation of  $L_e$ , depending on the inlet conditions. The parameters considered here are the inlet Froude and Reynolds numbers ( $Fr_0$  and  $Re_0$ ), the filling ratio at the inlet ( $h_0/D$ ), and the pipe slope ( $S$ ). This study also differs from previous studies in that control parameters such as the Reynolds and Froude numbers are calculated at the channel inlet section rather than in the uniform flow region.

In Fig. 10, the variation of the flow depth,  $h$ , in the streamwise direction on the symmetry plane is presented for the case of which the velocity profiles are plotted in Fig. 9. The curve  $h = h(x)$  asymptotically approaches a constant value  $h = h_n = 0.119$  m up to a certain distance upstream the overfall, where the subscript “ $n$ ” denotes uniform flow condition, and  $h_n$  is the normal depth.

Definition of quantities exhibiting asymptotic behavior is generally based on a limiting value, considering to what degree that limit is approached. For example, boundary layer thickness is defined as the perpendicular distance from the wall at which the velocity reaches 99% of the free-stream velocity [28]. Similarly, Durst et al. [29] defined the entrance length in laminar pipe flow as the distance at which the centerline velocity reaches 99% of its fully developed value. However, a similar criterion has not been proposed in the literature for the length of

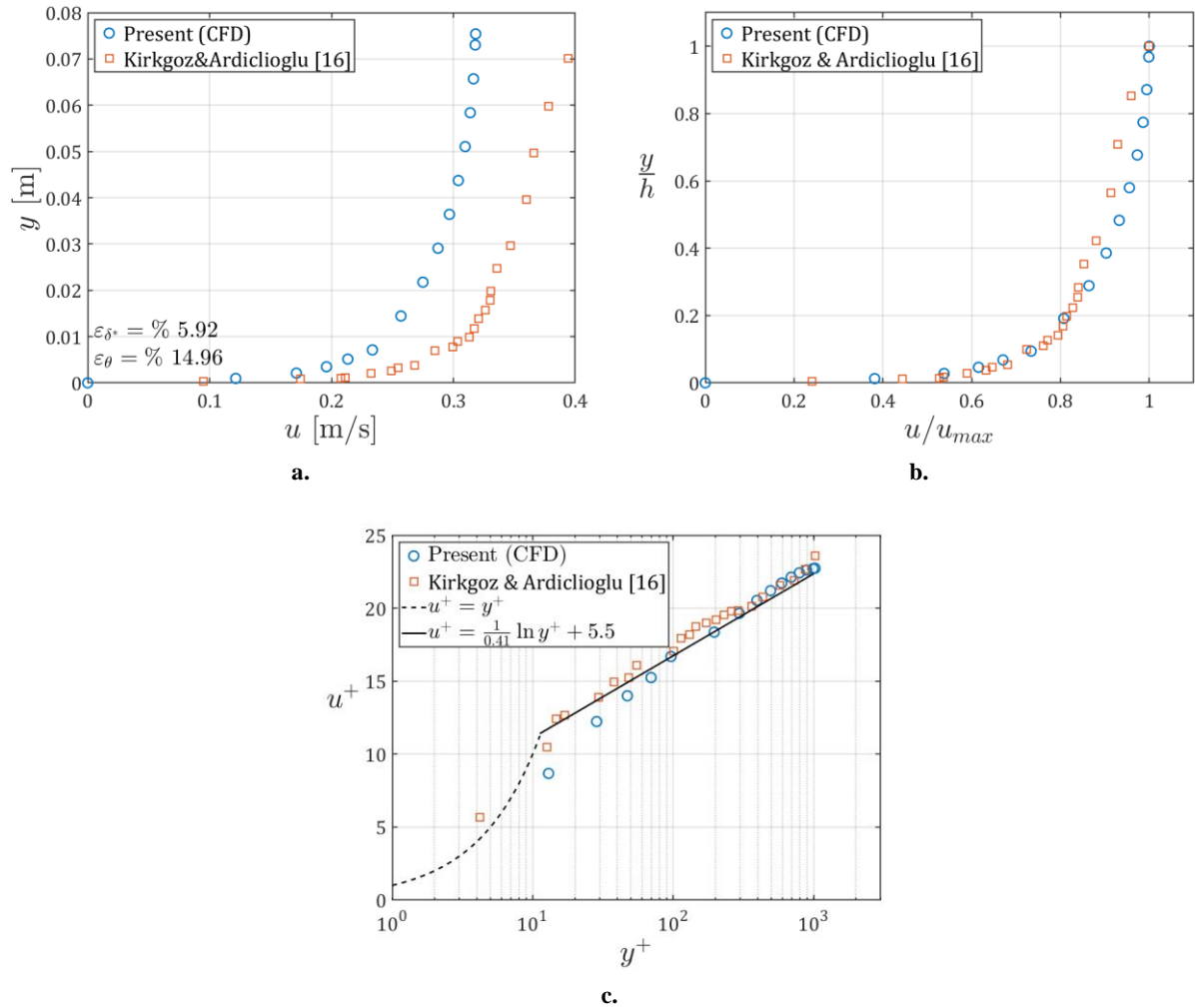


**Figure 8.** Comparison of the numerical and experimental a) velocity profiles at a uniform open-channel cross-section, b) velocity profiles nondimensionalized by mean flow variables  $u_{max}$  and  $h$ , and c) velocity profiles nondimensionalized by the wall variables, along with the logarithmic law of the wall

the transitory zone ( $L_e$ ) in open-channel flow. Kirkgoz and Ardicioglu [16] stated that they determined the flow development length by comparing velocity profiles at different cross-sections. However, as seen in Fig. 9, using this method would not be reliable in this case. The velocity profiles presented by Ead et al. [30] for uniform open-channel flow in a corrugated pipe also exhibit a similar variation to that shown in Fig. 10. Moreover, that study does not provide information regarding the streamwise distance over which the flow evolves to uniform flow.

Since determining the onset of uniform flow based on the criterion of an invariant velocity profile is not a practical method, this study considers the limit value of flow depth approached in the streamwise direction, which is the normal depth,  $h_n$ ; and the corresponding normal velocity,  $U_n$ . Thus, in this study, the length of the transitory zone,  $L_e$ , refers to the distance between the pipe inlet and the downstream location where the conditions of either  $U = 0.98U_n$  (for subcritical inlet) or  $U = 1.02U_n$  (for supercritical inlet) is satisfied for the cross-sectional

average velocity,  $U$ , provided that the velocity profile at the pipe entrance is uniform.

Table 4 and 5 present results for variation in the dimensionless length of the transitory zone ( $L_e/D$ ) with several parameters specified at the pipe inlet such as the filling ratio ( $h_0/D$ ), the Froude number ( $Fr_0$ ), Reynolds number ( $Re_0$ ), average velocity ( $U_0$ ); as well as slope ( $S$ ) and diameter ( $D$ ) for open channel flow in circular smooth and corrugated pipes, respectively. Comparing the values of  $L_e/D$  for the smooth pipe cases S1, S8, S9 and S10 indicates that there is an uncertainty of approximately 5% in the numerical solutions, since no change with the pipe diameter ( $D$ ) is expected while all the other parameters are kept constant. Smaller values of  $L_e/D$  are observed compared to those of the smooth case, which can be explained by the well-known fact, that turbulent boundary layer becomes fully developed in a shorter distance on a rough surface than it does on a smooth one [28].

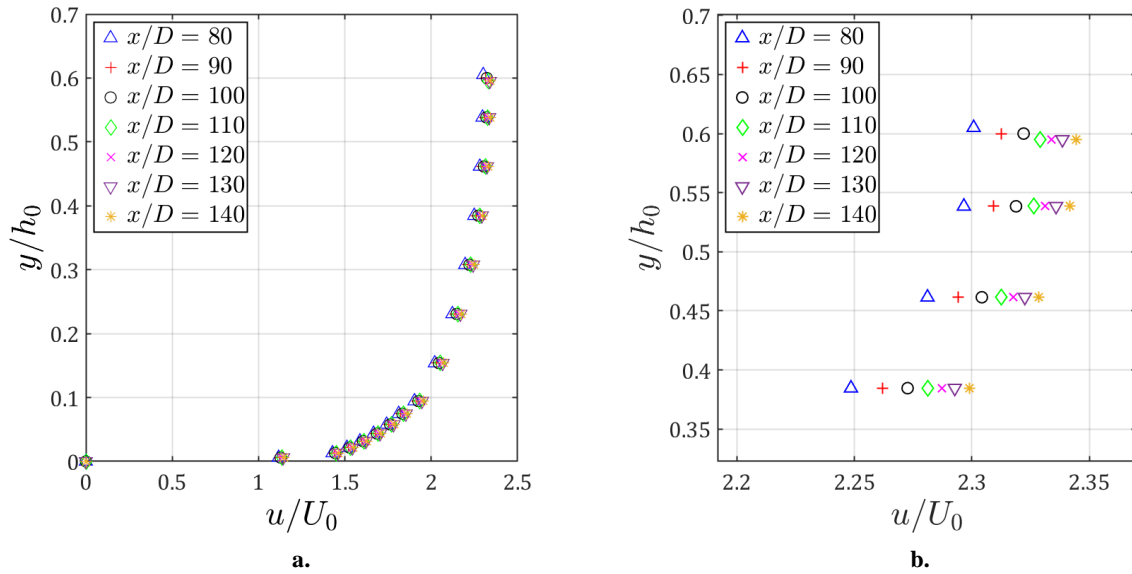


**Figure 9.** Streamwise development of axial velocity profiles in open channel flow in smooth pipe: a) general, and b) detailed view

### 3.1. Effect of the Reynolds and Froude Numbers

Fig. 11a shows results of the numerical solutions related to the dimensionless length of the transitory zone ( $L_e/D$ ) in smooth circular pipe for three different values of Reynolds number ( $Re_0$ ), and Froude numbers of  $Fr_0 = 0.8$ , 2.3 and 2.6. Accordingly, the variation of  $L_e/D$  with  $Re_0$  has quite different functional forms for the Froude numbers considered. It can be observed that an inverse proportionality between  $L_e/D$  and  $Re_0$  exists for  $Fr_0 = 2.3$ , and partly for  $Fr_0 = 2.6$  (Fig. 11a). This is consistent with the results of the experimental and numerical studies of Kirkgoz and Ardicioglu [16] and Bonakdari et al. [18], respectively. However, for sub-critical inlet condition ( $Fr_0 = 0.8$ ), variation in  $L_e/D$  is negligible: since it does not exceed the uncertainty level of the numerical solutions, which is found to be 5%. Fig. 11b indicates that present data for  $Fr_0 = 2.3$  in corrugated pipe seem to follow a line with negative slope, while change in  $L_e/D$  with  $Re_0$  is negligible for  $Fr_0 = 0.8$  and  $Fr_0 = 1.6$ . The

latter contradicts with the numerical results obtained by Bonakdari et al. [18] for rough rectangular channels, as they claim a linear decrease in flow development length with the Reynolds number. Nevertheless, Ranga Raju et al. [17] observed no variation with the Reynolds and Froude numbers in their numerical study for rough rectangular channel.

Fig. 12a illustrates variation of  $L_e/D$  with the Froude number ( $Fr_0$ ) for three different values of the Reynolds number,  $Re_0$ , in circular smooth pipe. It can be seen that while variation in  $L_e/D$  is negligible for  $Fr_0 < 2.3$  and  $Re_0 = 3.5 \times 10^4$ , there is a significant increase in  $L_e/D$ , as  $Fr_0$  rises to 2.6. For  $Re_0 = 10^5$  and  $3.5 \times 10^5$ , however, there is an inflection point at around  $Fr_0 = 2$ , where  $L_e/D$  has its minimum value, where  $L_e/D$  decreases for  $Fr_0 < 2$  and increases with a relatively much steeper slope for  $Fr_0 > 2$ . Thus, it can be concluded that data representing the variation of  $L_e/D$  with Froude number almost collapse onto a single curve at high Reynolds numbers ( $Re_0 \geq 10^5$ ).

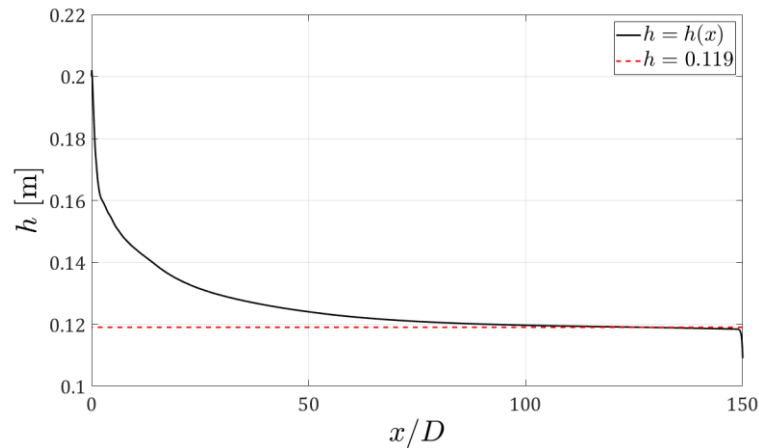


**Figure 10.** Streamwise variation of the flow depth in open channel flow in smooth pipe

**Table 4.** Variation of the dimensionless transitory length ( $L_e/D$ ) with inlet conditions for open-channel flow in circular smooth pipe

Case	$D$ (m)	$h_0/D$	$Fr_0$	$U_0$ (m/s)	$S$	$Re_0$	$L_e/D$
S1			0.8	0.693			64
S2	0.2	0.5	1.6	1.404	0.01	$3.5 \times 10^4$	63
S3			2.3	1.981			63
S4			2.6	2.282			91
S5			0.8	0.693			70
S6	0.2	0.5	2.3	2.019	0.01	$3.5 \times 10^5$	2
S7			2.6	2.282			87
S8			0.1	0.490			62
S9	0.4	0.5	0.8	0.981	0.01	$3.5 \times 10^4$	68
S10	0.6			1.201			66
S11	0.2	0.2	0.8	0.438	0.01	$3.5 \times 10^4$	59
S12		0.7	0.841	78			
S13					0.002		7
S14	0.2	0.5	0.8	0.693	0.005	$3.5 \times 10^4$	29
S15					0.02		62
S16					0.04		63
S17					0.8		0.693
S18			1.8	1.580			66
S19	0.2	0.5	2.0	1.756	0.01	$1.0 \times 10^5$	51
S20			2.3	1.981			57
S21			2.6	2.282			108
S22			3.0	2.633			134

The functional form of  $L_e/D$  in corrugated pipe is similar to that of smooth pipe, whereas the inflection point is around  $Fr_0 = 1.6$  (Fig. 12b). Contrary to the results of the present study for smooth and rough channels with circular cross-section, numerical studies of Ranga Raju et al. [17] and Bonakdari et al. [18] for open channel flow in smooth and rough rectangular channels imply no Froude number dependence.

### 3.2. Effect of the Filling Ratio

Values of  $L_e/D$  for pipe inlet filling ratios of  $h_0/D = 0.2, 0.5$  and  $0.7$  ( $Fr_0 = 0.8$  and  $Re_0 = 3.5 \times 10^4$ ) are plotted in Fig. 13a for open channel flow in smooth circular pipe. Considering only the data presented herein, it can be stated that variation of  $L_e/D$  with  $h_0/D$  is a non-linear increasing function. As for the corrugated pipe, variation of  $L_e/D$  can be approximated by a linear function with positive slope, instead (Fig. 13b). Further numerical calculations are needed to investigate the effect of the filling ratio for different values of  $Fr_0$  and  $Re_0$ .

### 3.3. Effect of Slope

A plot of the dimensionless length of the transitory zone ( $L_e/D$ ) versus pipe slope ( $S$ ) can be seen in Fig. 14a for slopes of  $S = 0.002, 0.005, 0.01, 0.02, 0.03$  and  $0.04$  in smooth circular pipe. According to the results for smooth pipe, the variation of  $L_e/D$  is not larger than the uncertainty level of 5% for  $0.01 \leq S \leq 0.04$  and it can be assumed to be constant within this range of slope for  $Fr_0 = 0.8$  and  $Re_0 = 3.5 \times 10^4$ . However, there is a rapid change in  $L_e/D$  for  $S < 0.01$ , which can be approximated by a linear function with a steep slope. For open channel flow in corrugated pipe,  $L_e/D$  falls rapidly for  $S < 0.005$  and then approaches asymptotically to a constant value (Fig. 14b). Overshoot and undershoot in the curves representing the variation of  $L_e/D$  is evident for smooth and corrugated circular pipes, respectively.

**Table 5.** Variation of the dimensionless transitory length ( $L_e/D$ ) with inlet conditions for open-channel flow in circular corrugated pipe

Case	$D$ (m)	$h_0/D$	$Fr_0$	$U_0$ (m/s)	$S$	$Re_0$	$L_e/D$
C1			0.8	0.693			21
C2	0.2	0.5	1.0	0.878	0.01	$3.5 \times 10^4$	19
C3			1.6	1.404			4
C4			2.3	1.981			48
C5			0.8	0.693			21
C6	0.2	0.5	1.6	1.404	0.01	$1.0 \times 10^5$	4
C7			2.3	1.981			43
C8			3.0	2.971			53
C9			0.1	0.490			15
C10	0.4	0.5	0.8	0.981	0.01	$3.5 \times 10^4$	21
C11	0.6			1.201			22
C12					0.002		54
C13	0.2	0.5	0.8	0.693	0.005	$3.5 \times 10^4$	10
C14					0.02		25
C15					0.04		24

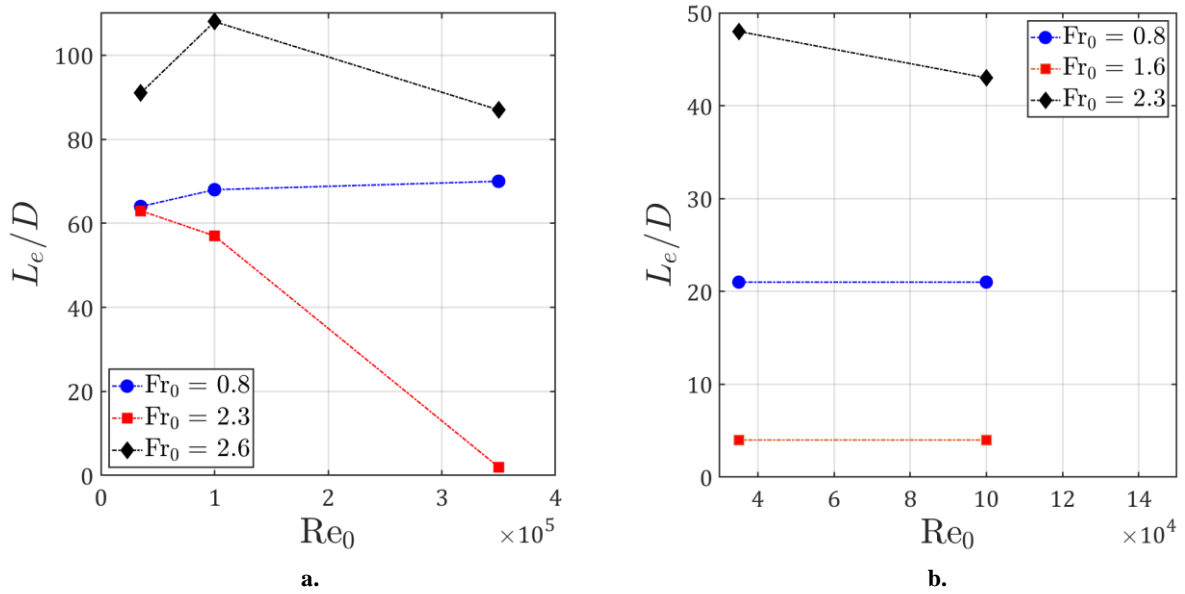


**Figure 11.** Variation of  $L_e/D$  with Reynolds number at three different Froude numbers for open channel flow in a) smooth and b) corrugated pipe

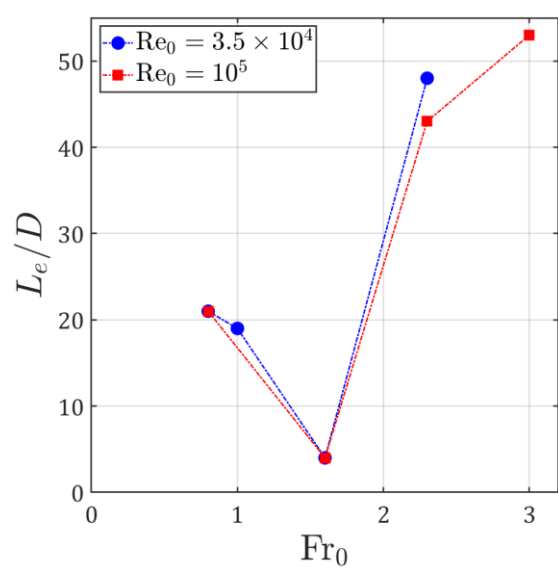
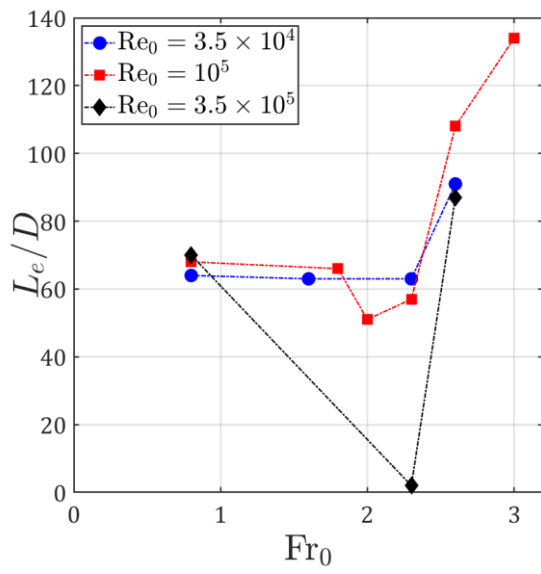


**Figure 12.** Variation of  $L_e/D$  with Froude number at different Reynolds numbers for open channel flow in a) smooth and b) corrugated pipe

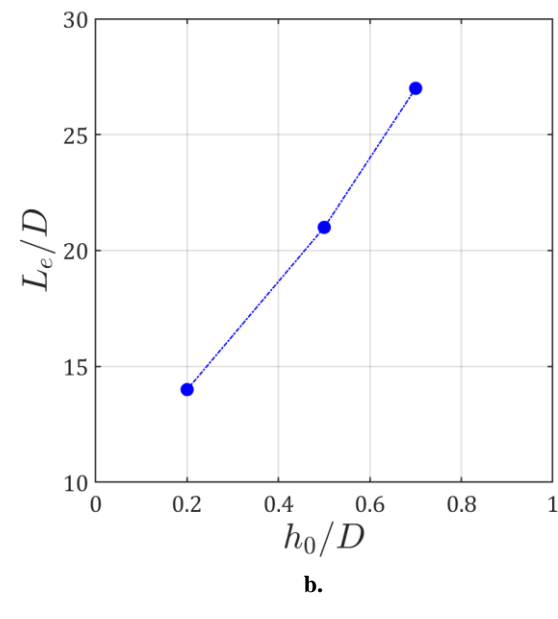
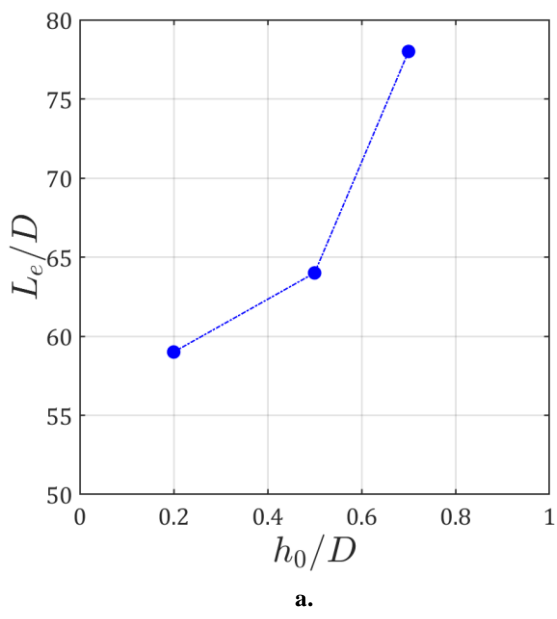


**Figure 13.** Variation of  $L_e/D$  with pipe filling ratio ( $h_0/D$ ) at  $Fr_0 = 0.8$  and  $Re_0 = 3.5 \times 10^4$ , for open channel flow in a) smooth and b) corrugated pipe

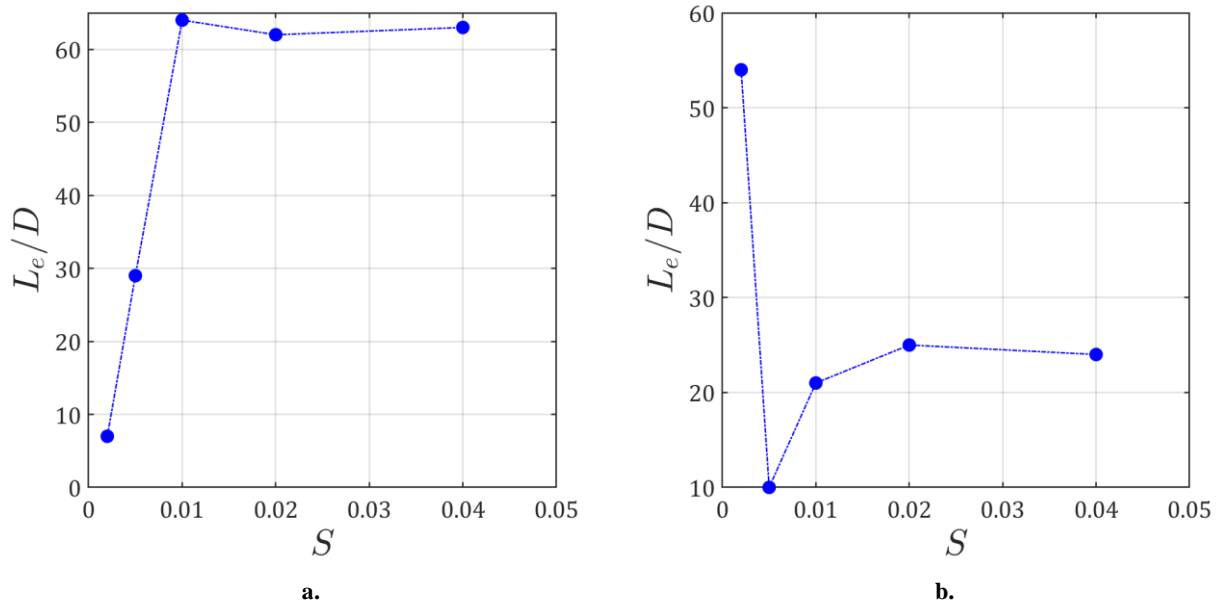


**Figure 14.** Variation of  $L_e/D$  with channel slope ( $S$ ) for  $Fr_0 = 0.8$  and  $Re_0 = 3.5 \times 10^4$ , for open channel flow in a) smooth and b) corrugated pipe

#### 4. CONCLUSION

Numerical calculations are conducted to be able to assess variation of the length of the transitory zone ( $L_e/D$ ) for open channel flow in smooth and corrugated circular pipes with parameters such as the Reynolds and Froude numbers, filling ratio and pipe slope. Results of the present study show that, considering that variation of the entry length with Reynolds number is an increasing function for turbulent pipe flow; the situation for open channel generally seems to be quite the opposite, as the transitory length exhibits a tendency to decrease with the Reynolds number. Furthermore, it is concluded that  $L_e/D$  dramatically changes with the Froude number, as well as with the filling ratio. Significant variation in  $L_e/D$  is observed only for values of channel slope smaller than 0.001. Aside from the distinct cross-sectional geometry of the channel, a significant distinction of the present study from the previous studies cited herein is specification of the related parameters, such as the Reynolds and Froude numbers, at the channel inlet, rather than in the uniform flow region. In fact, the numerical results presented herein should be regarded just as a rough estimation for the length of the transitory zone; since both the turbulence model and the grid used, as well as the wall functions employed, are not capable of capturing the transition of boundary layer from laminar to turbulent in the developing flow region.

#### DECLARATION OF COMPETING INTEREST

The authors declare that they have no known competing financial interests or personal relationships that could have appeared to influence the work reported in this paper.

#### DECLARATION OF ETHICAL STANDARDS

The author(s) of this article declare that the materials and methods used in this study do not require ethical committee permission and/or legal-special permission.

#### AUTHORS' CONTRIBUTIONS

**Kenan KAYA:** Validation, Investigation, Data Curation, Formal Analysis, Writing-original draft, Writing – review & editing, Visualization.

**Öktay ÖZCAN:** Supervision, Conceptualization, Methodology, Writing – original draft, Visualization, Data curation.

#### REFERENCES

- [1] Chow, V. T., “*Open-channel hydraulics*”, McGraw-Hill, New York, (1959).
- [2] Shah, R. K., and London, A. L., “*Laminar Flow Forced Convection in Ducts: A Source Book for Compact Heat Exchanger Analytical Data*”, Academic Press, New York, (1978).
- [3] Patel, R. P., “A note on fully developed turbulent flow down a circular pipe”, *Aeronaut. J.*, 78(758-759), 93-97, (1974).
- [4] Nezu, I. and Rodi, W., “Open-channel flow measurements with a laser doppler anemometer”, *J. Hydraul. Eng.*, 112(5), 335-355, (1986).
- [5] Balachandar, R., Blakely, D., Tachie, M., and Putz, G., “A study on turbulent boundary layers on a smooth flat plate in an open channel”, *J. Fluids Eng.*, 123(2), 394-400, (2001).
- [6] Das, S., Balachandar, R., and Barron, R. M., “Generation and characterization of fully developed state in open

- channel flow”, *Journal of Fluid Mechanics*, 934, A35, (2022).
- [7] Tominaga, A., Nezu, I., Ezaki, K., and Nakagawa, H., “Three-dimensional turbulent structure in straight open channel flows”, *J. Hydraul. Res.*, 27(1), 149-173, (1989).
- [8] Knight, D. W., “Boundary shear in circular pipes running partially full”, *J. Hydraul. Eng.*, 126(4), 263-275, (2000).
- [9] Subramanya, K., “*Flow in open channels*”, McGraw-Hill, New Delhi, India, (1994).
- [10] Carstens, M. R. and Carter, R. W., “Discussion on “Hydraulics of free overfall” by A. Fathy and M. A. Shaarawi. *Proc. Amer. Soc. Civil Eng.*, 91(HY3), 149-163, (1955).
- [11] Bos, M. G., “*Discharge measurement structures*”, 3rd Ed., Publication 20, Int. Institute for Land Reclamation and Improvement/ILRI, Wageningen, The Netherlands, (1989).
- [12] Ferro, V., “Flow Measurement with Rectangular Free Overfall”, *J. Irrig. Drain. Eng.*, 118(6): 956-964, (1992).
- [13] Tokyay, N. D., and Yildiz, D., “Characteristics of free overfall for supercritical flows”, *Can. J. Civ. Eng.*, 34(2), 162-169, (2007).
- [14] Bauer, S.W., and Graf, W.H., “Free overfall as flow measuring device”, *Journal of Irrigation and Drainage Division*, ASCE, 97(1), 73–83, (1971).
- [15] Rajaratnam, N., and Muralidhar, D., “End depth for circular channels”, *Journal of the Hydraulics Division*, 90(2), 99-119, (1964).
- [16] Kirkgöz, M. S. and Ardiclioglu, M. “Velocity profiles of developing and developed open channel flow”, *J. Hydraul. Eng.*, 123(12), 1099-1105, (1997).
- [17] Ranga Raju, K. G., Asawa, G. L. and Mishra, H. K., “Flow-Establishment Length in Rectangular Channels and Ducts”, *J. Hydraul. Eng.*, 126(7): 533-539, (2000).
- [18] Bonakdari, H., Lipeme-Kouyi, G. and Asawa, G. L., “Developing turbulent flows in rectangular channels: A parametric study”, *J. Appl. Res. Water Wastewater*, 1(2), 53-58, (2014).
- [19] Wilkerson, G., Sharma, S. and Sapkota, D., “Length for Uniform Flow Development in a Rough Laboratory Flume”, *J. Hydraul. Eng.*, 145(1), 06018018, (2019).
- [20] Hyman, J. M. “Numerical Methods for Tracking Interfaces”, *Physica D*, 12(1-3): 396-407., (1984).
- [21] McKee, S., Tome, M. F., Ferreira, V. G., Cuminato, J. A., Castelo, A., Sousa, F. S. and Mangiavacchi, N. “The MAC Method”, *Comput. Fluids*, 37: 907-930., (2008).
- [22] Hirt, C. W., and Nichols, B. D., “Volume of Fluid Method for the Dynamics of Free Boundaries”, *J. Comput. Phys.*, 39: 201-225., (1981).
- [23] Hirsch, C., “*Numerical Computation of Internal and External Flows*”, John Wiley & Sons, (1988).
- [24] Harten, A., “High Resolution Schemes for Hyperbolic Conservation Laws”, *J. Comput. Phys.*, 49(3): 357-393, (1983).
- [25] Muzaferija, S., Peric M., Sames, P. and Schelin, T., “A Two-fluid Navier-Stokes Solver to Simulate Water Entry”, *Proceedings of Twenty-Second Symposium on Naval Hydrodynamics*, 277-289, Washington, DC, (1998).
- [26] Ubbink, O. “*Numerical Prediction of Two Fluid Systems with Sharp Interfaces*”, PhD Thesis, Imperial College of Science, Technology and Medicine, London, England, (1997).
- [27] Menter, F. R., “Two-equation Eddy-viscosity Turbulence Models for Engineering Applications”, *AIAA J.*, 32(8): 1598-1605, (1994).
- [28] Schlichting, H., “*Boundary Layer Theory*”, McGraw-Hill Book Company, New York, (1979).
- [29] Durst, F., Ray, S., Ünsal, B. and Bayoumi, O. A., “The Development Lengths of Laminar Pipe and Channel Flows”, *J. Fluids Eng.*, 127(6): 1154-1160, (2005).
- [30] Ead, S. A., Rajaratnam, N., Katopodis, C. and Ade, F., “Turbulent Open-Channel Flow in Circular Corrugated Culverts”, *J. Hydraul. Eng.*, 126(10): 750-757, (2000).